AGU PUBLICATIONS

Geophysical Research Letters

Key Points:
- Labile-particulate iron has a key role in iron cycling and can increase the overall "available" iron pool by up to 55% in the OMZ
- A strong relationship between particles and dissolved iron indicates that L-pFe "buffers" the elevated dFe concentrations observed
- Lateral shelf transport of available Fe (L-pFe + dFe) supplied a similar magnitude of iron as atmospheric sources

Supporting Information:
- Supporting Information S1
- Figure S1
- Figure S2
- Figure S3

Correspondence to:
A. Milne,
angela.milne@plymouth.ac.uk

Particulate phases are key in controlling dissolved iron concentrations in the (sub)tropical North Atlantic

Angela Milne[1] , Christian Schlosser[2,3] , Bronwyn D. Wake[2] , Eric P. Achterberg[2,3] , Rosie Chance[4,5] , Alex R. Baker[4] , Alex Forryan[2], and Maeve C. Lohan[1,6]

[1]School of Geography, Earth and Environmental Sciences, Plymouth University, Plymouth, UK, [2]Ocean and Earth Sciences, National Oceanography Centre, University of Southampton, Southampton, UK, [3]GEOMAR Helmholtz Centre for Ocean Research, Kiel, Germany, [4]Centre for Ocean and Atmospheric Sciences, School of Environmental Sciences, University of East Anglia, Norwich, Norfolk, UK, [5]Now at Department of Chemistry, University of York, Heslington, York, UK, [6]Now at Ocean and Earth Sciences, National Oceanography Centre, University of Southampton, Southampton, UK

Abstract The supply and bioavailability of iron (Fe) controls primary productivity and N_2 fixation in large parts of the global ocean. An important, yet poorly quantified, source to the ocean is particulate Fe (pFe). Here we present the first combined dataset of particulate, labile-particulate (L-pFe), and dissolved Fe (dFe) from the (sub)tropical North Atlantic. We show a strong relationship between L-pFe and dFe, indicating a dynamic equilibrium between these two phases whereby particles "buffer" dFe and maintain the elevated concentrations observed. Moreover, L-pFe can increase the overall "available" (L-pFe + dFe) Fe pool by up to 55%. The lateral shelf flux of this available Fe was similar in magnitude to observed soluble aerosol-Fe deposition, a comparison that has not been previously considered. These findings demonstrate that L-pFe is integral to Fe cycling and hence plays a role in regulating carbon cycling, warranting its inclusion in Fe budgets and biogeochemical models.

1. Introduction

Iron (Fe) is an essential micronutrient for the growth of phytoplankton and hence plays a crucial role in ocean ecosystems [*Boyd and Ellwood*, 2010]. It is required for key metabolic functions such as photosynthesis and nitrogen (N_2) fixation [*Morel et al.*, 2003; *Sunda*, 2001; *Whitfield*, 2001]. The sensitivity of ecosystems to Fe supply is related to its short residence time, which is in the order of days to months in surface waters and tens to a few hundred years in deep waters [*Bergquist et al.*, 2007; *Bruland et al.*, 1994]. The dissolved phase (dFe) is considered the most biologically available fraction [*Wells et al.*, 1995]; however, the main flux of Fe to the ocean is in the particulate form (i.e., dust deposition, river transport, sediment resuspension, off-shelf transport and ice-rafted debris). The oceanic Fe inventory in shelf systems is dominated by the particulate phase (pFe) [*Hong and Kester*, 1986; *Lippiatt et al.*, 2010], yet the cycling of this fraction in shelf or open ocean environments is not well constrained. In oxygenated seawater, the predominant Fe species, Fe(III), is highly insoluble and precipitates to form particulate phases [*Sunda*, 2001; *Wu and Luther*, 1994]. This process is mitigated by the presence of natural organic ligands which complex ~99% of dFe and hence regulate dFe concentrations [*Gledhill and van den Berg*, 1994; *Rue and Bruland*, 1995]. Scavenging and precipitation of Fe to particulate phases result in losses of dFe. However, a surface-bound labile-pFe (L-pFe) fraction is considered to be involved in adsorption/desorption processes [*Homoky et al.*, 2012] with Fe becoming available to phytoplankton following dissolution and solubilization [*Hurst et al.*, 2010; *Lippiatt et al.*, 2010]. This fraction can include acid-labile hydroxides and biogenic particles as well as surface-bound forms of Fe. Scavenging and dissolution interactions between L-pFe and dFe, plus remineralization from biogenic particles, may govern the distribution of dFe in the ocean.

In the North Atlantic, mineral dust forms the principal source of soluble and bioavailable Fe to surface waters [*Jickells et al.*, 2005; *Schlosser et al.*, 2014]. Additionally, continental margins and shelf sediments are significant sources of Fe to the ocean [*Elrod et al.*, 2004; *Lam and Bishop*, 2008] and can dominate the Fe budget on a global scale [*Tagliabue et al.*, 2014]. Inputs of particulate material from margins and Fe from enriched pore waters not only sustain productivity in shallow coastal waters [*Hurst et al.*, 2010] but also supply Fe to the ocean interior, either through lateral advection [*Lam et al.*, 2006] or mesoscale eddy transport [*Boyd et al.*, 2012; *Lippiatt et al.*, 2011].

We quantified the distributions of L-pFe, pFe, and dFe in the (sub)tropical northeast Atlantic and explored the role of particles on the distribution of dFe. Atmospheric deposition [*Ohnemus and Lam*, 2015; *Powell et al.*, 2015], lateral advection of Fe from the eastern continental margin [*Conway and John*, 2014; *Rijkenberg et al.*, 2012], and inputs from benthic nepheloid layers [*Lam et al.*, 2015] all supply particulate Fe to this region. Here we present the first combined dataset of these three Fe fractions.

2. Materials and Methods

2.1. Sample Collection and Pretreatment

Samples were collected during the GEOTRACES GA06 section in the (sub)tropical Northeast Atlantic (Figure 1a) from 7 February to 19 March 2011. Particulate samples were collected onto acid clean 25 mm Supor® poly-ethersulfone membrane disc filters (Pall, 0.45 μm) and stored frozen (−20°C) until shore-based analysis. Seawater samples were filtered using 0.8/0.2 μm cartridge filters (AcroPak500/1000^TM), acidified to 0.013 M with high purity HCl (Romil, UpA) and allowed to equilibrate for at least 24 h prior to onboard analysis. In a land-based laboratory, the labile-particle fraction of Fe and aluminum (Al) was determined using the protocol of *Berger et al.* [2008]. For determination of total pFe and pAl, a sequential acid digestion modified from *Ohnemus et al.* [2014] was used. Full details are in supporting information Methods 1.

2.2. Sample Analyses

All particle samples were analyzed using inductively coupled plasma-mass spectrometry (Thermo Fisher XSeries-2). Potential interferences (e.g., $^{40}Ar^{16}O$ on ^{56}Fe) were minimized through the use of a collision/reaction cell utilizing 7% H in He. Evaluation of the leach and digestion efficiencies was made using four certified reference materials with the results showing good agreement (Table S1). Dissolved Fe was determined using flow-injection analysis with chemiluminescence detection [*Klunder et al.*, 2011; *Obata et al.*, 1993].

2.3. Atmospheric Sampling and Analysis

Clean aerosol samples were collected using a high volume (~1 m^3 min^{-1}) collector equipped with a three-stage Sierra-type cascade impactor head. Sample filters were stored frozen (−20°C) until shore-based analysis. Soluble aerosol Fe and Al were determined as detailed in *Baker et al.* [2007]. Total Fe and Al were determined by instrumental neutron activation analysis following protocols detailed in *Baker et al.* [2013]. Concentrations were converted to dry deposition fluxes by multiplying by the deposition velocity (V_d). Soluble aerosol concentrations were multiplied by a wind-speed dependent value of V_d (calculated using the method of *Ganzeveld et al.* [1998]) assuming an aerodynamic diameter of 5 μm for the coarse mode (sampling cutoff of >1 μm) and 0.6 μm for the fine mode (cutoff of <1 μm). Total aerosol Fe and Al concentrations were only determined for bulk aerosol, and so a single value of V_d (0.3 cm s^{-1}) was used. Further details are in supporting information Methods 2.

2.4. Horizontal Fluxes and Vertical Eddy Diffusivity

The offshore horizontal flux of Fe was estimated from the averaged decreasing concentrations, moving away from the continental shelf, taken from depths below the mixed layer to 500 m. The same potential density gradients were followed from the coast to the open ocean and encompassed the highest concentrations of dFe in the oxygen minimum zone (OMZ). To calculate estimates of the horizontal flux, a simplified one-dimensional advective/diffusion model, $\frac{\partial(Fe)}{\partial t} = -u\left(\frac{\partial(Fe)}{\partial x}\right) + K_h\left(\frac{\partial x^2(Fe)}{\partial x^2}\right) + J_h$, was applied [*de Jong et al.*, 2012; *Glover et al.*, 2011]. The vertical flux of Fe (J_Z) in the upper water column was calculated as detailed in *Jickells* [1999] following the equation $J_Z = w\lceil Fe\rceil_{BML} + K_Z\frac{\partial Fe}{\partial z}$. Full details can be found in supporting information Methods 3 [*Duce et al.*, 1986; *Neuer et al.*, 1997; *Okubo*, 1971; *Rhein et al.*, 2010; *Stramma et al.*, 2008; *Stramma et al.*, 2005; *Stramma and Schott*, 1999].

3. Results and Discussion

3.1. Distribution and Sources of Fe

Maximum concentrations of pFe (up to 140 nM), and pAl (up to 800 nM) as an indicator of mineral particle input [*Duce et al.*, 1991], were observed close to the continental margin while elevated values occurred across the full extent of the shelf slope (pFe: 10–50 nM, pAl: 50–200 nM; Figures 1b–1c). A key feature of our study area is the
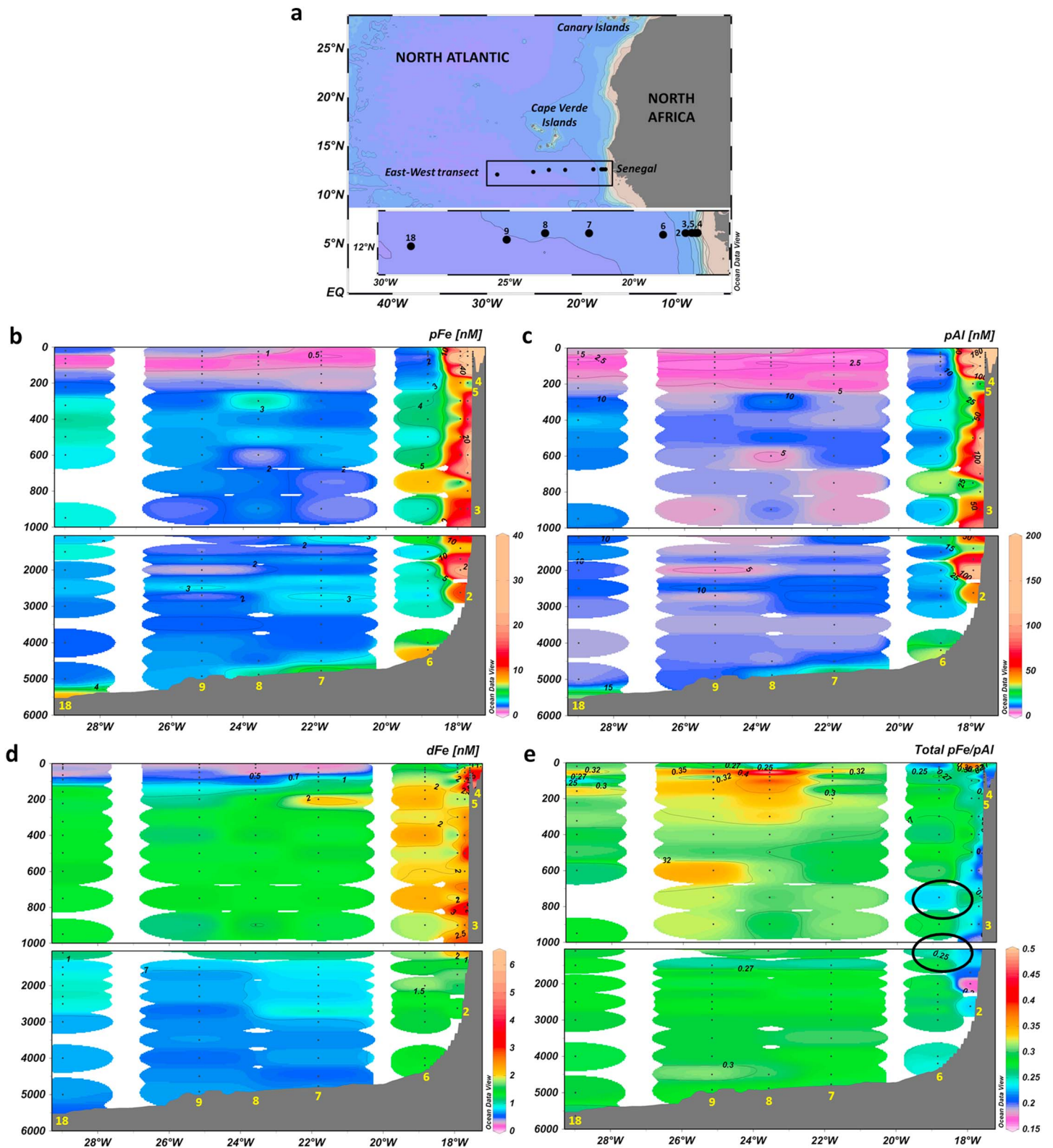
Figure 1. Location and profiles from GEOTRACES A06 Cruise. (a) The transect and sampling stations, (b) pFe, (c) pAl, (d) dFe, and (e) ratio of pFe/pAl with INLs at station 6 circled. Stations noted in yellow. Plots produced using Ocean Data View (Schlitzer, R., http://odv.awi.de).

oxygen minimum zone (Fig. S1) which extends from ~100 to 1000 m and was associated with enhanced dFe concentrations >1 nM (Figure 1d). Neither the pFe nor the pAl distributions were influenced by low oxygen concentrations (41.2 to ~100 μmol kg^{-1}), indicating no influence on particle formation, dissolution, and cycling. Instead, particle distributions were controlled by input (continental margin/atmosphere) and removal (remineralization/sedimentation) processes as reported in previous studies of this region [*Ohnemus and Lam*, 2015; *Revels et al.*, 2015]. The observed pFe/pAl mole ratios in waters adjacent to the shelf (<100 km from the African coast) ranged between 0.17 and 0.21 (Figure 1e), values which are similar to upper crustal mole ratios (0.19–0.23 [*McLennan*, 2001; *Rudnick and Gao*, 2003; *Wedepohl*, 1995]). Interestingly, raised pFe (5–8 nM) and pAl (20–33 nM) concentrations, typical from intermediate nepheloid layers (INLs), were observed ~200 km from the coast at station 6. The pFe/pAl ratio in these two layers was 0.23 and 0.25 (Figure 1e), while the average water column ratio at station 6 was 0.27 ± 0.02 (n = 21). The low ratios in the INLs suggest that the higher pFe and pAl signals also originated from the shelf. The overall concentrations of pFe and pAl in the western water column were significantly lower (Mann-Whitney rank sum test, P < 0.001) than in the eastern stations (2–6), and their distribution through the water column was relatively uniform (pFe: 1–3 nM; pAl: 5–10 nM). Here, the pFe/pAl ratios were higher than the overall average values observed east of station 6, averaging 0.30 ± 0.04 (n = 80) compared to 0.25 ± 0.06 (n = 59). Neither set of values are statistically different to the mean Fe/Al mole ratio of 0.27 ± 0.04 (total dry deposition, n = 8) for our aerosol samples, which is also within the range previously reported for Saharan aerosols (0.26–0.37 [*Baker et al.*, 2013; *Formenti et al.*, 2003; *Shelley et al.*, 2015]). Large quantities of mineral dust are delivered to the North Atlantic through wet and dry deposition [*Baker et al.*, 2013; *Jickells et al.*, 2005; *Powell et al.*, 2015]. While no wet deposition was observed, dry deposition provided large and variable total (11,645 ± 5985 nmol m^{-2} d^{-1}) and soluble (112 ± 72 nmol m^{-2} d^{-1}) aerosol Fe fluxes (n = 8) which are typical for this region [*Rijkenberg et al.*, 2012; *Ussher et al.*, 2013]. This indicates that dust was a significant source of particulate material, in agreement with other studies of this region [*Conway and John*, 2014; *Revels et al.*, 2015].

3.2. Lability of Enriched pFe

Scavenging of dFe onto particles has been considered a loss from the dissolved "available" Fe pool, the consequences of which would be evident in the particulate fraction. Distinct enrichment of pFe over pAl, as indicated by raised pFe/pAl ratios (0.26–0.58; Figure 1e), was observed in subsurface waters (~25–50 m) at all stations except for the two coastal stations (4 and 5). This pFe enrichment coincided with depths of maximum fluorescence (Figure S2) and is indicative of both biological Fe uptake as well as scavenging. Moreover, enrichment of pFe (pFe/pAl > 0.32) was observed down to 400 m and to a lesser degree (pFe/pAl > 0.30) down to 1000 m, encompassing the OMZ in a similar manner to dFe (Figure 1e). The lability of the pFe fraction (Fig. S3) can provide an indication of the "available" particulate pool with a potential to impact dFe concentrations. Our results demonstrate that the Fe enrichment of particles was contained in the labile fraction, as indicated by the higher Fe/Al ratios observed for labile particles compared to the refractory component. The average refractory-pFe/pAl ratios in surface waters to the Chl *a* maximum, and down to 1100 m, were close to the upper crustal ratio (0.21 ± 0.02; n = 3 [*McLennan*, 2001; *Rudnick and Gao*, 2003; *Wedepohl*, 1995]; Figure 2a). In contrast, the average labile-pFe/pAl ratios at depths to the Chl *a* maximum were elevated (0.30–1.73; Figure 2a, upper panel). At depths down to 1100 m, this Fe enrichment was even more distinct, with labile-pFe/pAl ratios ranging from 0.81 to 1.58 (Figure 2a, lower panel), indicating increased Fe scavenging onto particles with depth. Overall, the leachable fraction (i.e., L-pFe/pFe × 100) ranged from 13% to 51% with a mean of 24% ±6.5 (n = 88) for all samples. A band of higher %L-pFe (~30%; Figure 2b) was evident in the upper water column (<400 m) where biological particle production and remineralization occurs. Indeed, positive correlations between L-pP and the biogenic elements of Cd (r^2 = 0.8278) and Co (r^2 = 0.8947) were also observed here, a further indication of biological processes. While overall, pFe predominantly correlated with pAl (r^2 = 0.9867) and pTi (r^2 = 0.9780), in agreement with previous studies [*Ohnemus and Lam*, 2015; *Twining et al.*, 2015], at depths down to the Chl *a* maximum, L-pFe revealed a minor positive correlation with L-pP (r^2 = 0.4176) indicating an association between L-pFe and biogenic matter in surface waters. At depths >400 m, %L-pFe decreased to ~20% which may indicate a change in the nature of the pFe (Figure 2b).

The distinct enrichment of L-pFe at the shelf stations (with labile-pFe/pAl ratios between 1.51 and 1.73; Figure 2a) was dramatically higher than at any other station. Productivity in the shelf region was at least twofold higher than at any other station, with Chl *a* concentrations reaching up to 5.9 μg L^{-1}. Coastal phytoplankton has a higher requirement for Fe compared to oceanic species and therefore store more Fe [*Brand*, 1991;
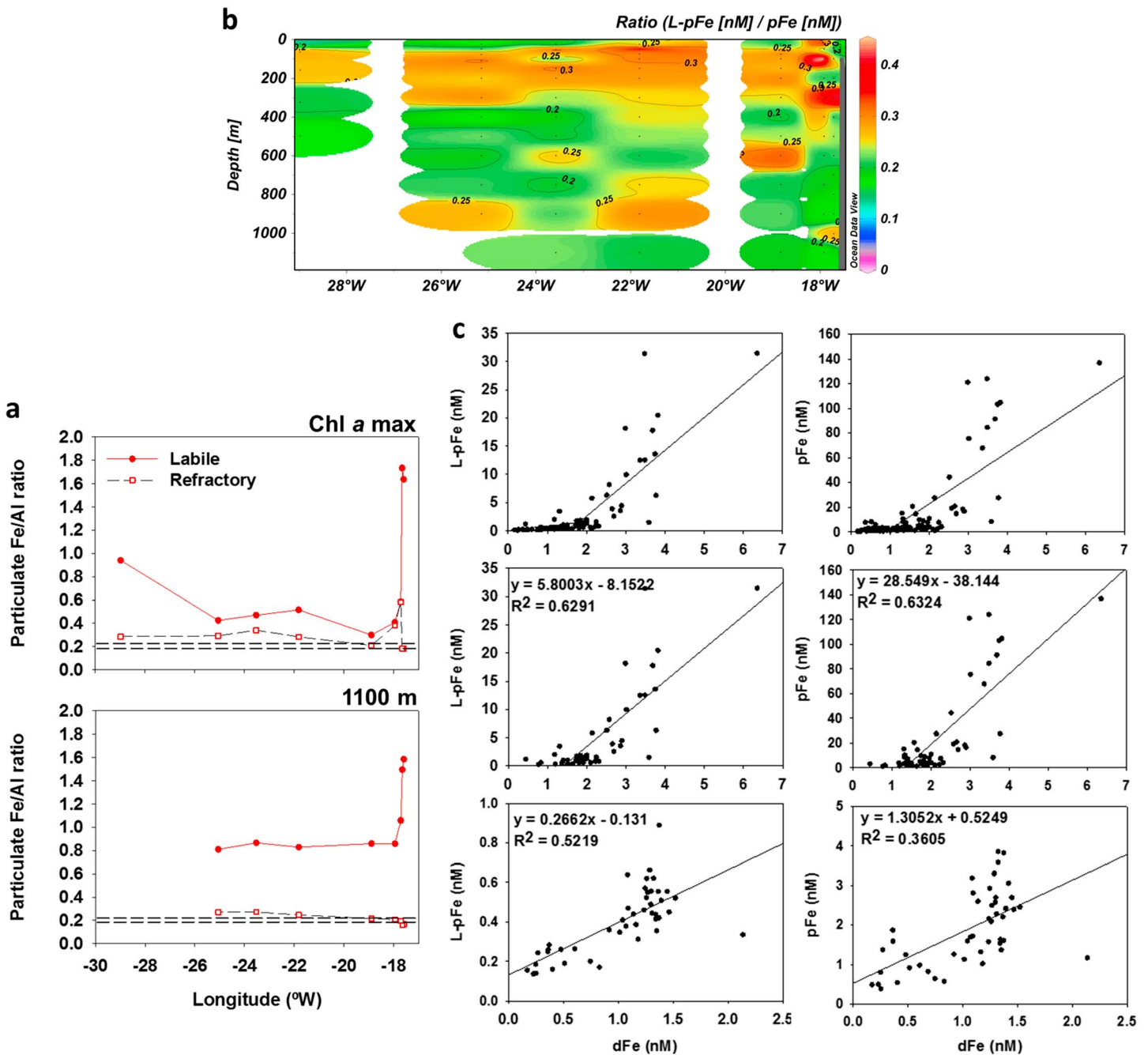
Figure 2. Labile-particulate Fe. (a) Enrichment of L-pFe (closed circles) over refractory-pFe (open squares) illustrated using Fe/Al ratios for the upper water column down to the Chl *a* maximum (upper panel) and from the bottom of the Chl *a* max to 1100 m (lower panel). The mol/mol crustal ratio range for Fe/Al (0.19–0.23) is indicated by dotted lines. (b) Distribution of L-pFe as a fraction of total pFe (L-pFe/pFe) in the upper 1100 m. (c) Relationship between dFe-L-pFe(left) and dFe-pFe(right) for all stations (upper), shelf-influenced stations 2–6 (middle) and open ocean stations 7–9 and 18 (bottom). Note change in scales in the bottom panels.

Maldonado and Price, 1996; *Marchetti et al.*, 2006; *Sunda et al.*, 1991]. The high productivity in conjunction with local planktonic species has resulted in Fe-rich biogenic particles. Furthermore, direct input of dFe from bottom sediments would subsequently be scavenged in the particle abundant shelf region. Dissolved Fe had a similar distribution to the pFe phases in the shelf region, with elevated concentrations reaching 4–6 n*M*. Furthermore, raised dFe concentrations (1.2–6.3 n*M*) persisted throughout the water column and were evident as far west as station 6, a trend also observed for pFe. These enhanced dFe concentrations are not associated with any changes in the physical properties of the water column and most likely

resulted from direct input of dFe from sediments and transport from the shelf [*Conway and John*, 2014] and/or dissolution from pFe.

3.3. Dynamic Equilibrium Between L-pFe and dFe

Comparison of pFe and L-pFe with dFe data in the OMZ revealed two distinct relationships as indicated by a "kink" (Figure 2c upper panels). Separating the stations into shelf influenced (stations 2–6, Figure 2c, middle panels) and open ocean (stations 7–9 and 18, Figure 2c, bottom panels) indicates strong positive correlations between L-pFe and dFe throughout the transect ($r^2 = 0.629$ and 0.522, respectively). While a strong positive correlation was evident between pFe and dFe at the shelf-influenced stations ($r^2 = 0.6324$), this was not similarly maintained in open ocean waters ($r^2 = 0.3605$) whereby less than 40% of the variability in pFe could be explained by dFe. The change in slopes between shelf-influenced and open ocean waters reflects the differing oceanic environments; for example, a rise of 5.8 nM L-pFe nM^{-1} dFe would be expected at shelf-influenced stations, in contrast to just 0.3 nM L-pFe nM^{-1} dFe in the open ocean, indicating a particle active regime closer to the shelf. This explains the strong relationship between both particle fractions and dFe in shelf-influenced waters. Away from the shelf, while a strong relationship still exists, the changes in pFe concentrations are less correlated with those of dFe. However, regardless of region, concentrations of pFe dominate over those of dFe, thus enabling L-pFe to be an important conduit between pFe and the "available" Fe pool. A recent model for the upper North Atlantic suggested that rates of sorption/desorption from particles were faster than biological uptake and remineralization rates [*John and Adkins*, 2012]. In our study region, there is a large pool of pFe with supply from both shelf (Figure 1b) and atmospheric sources. The relationships between L-pFe and dFe suggests that the two phases are intimately linked, most likely through dissolution and scavenging processes, resulting in an equilibrium; i.e., where there is high L-pFe, exchange mechanisms with the dissolved phase can occur resulting in high dFe concentrations and vice versa. Indeed, the distribution of dFe along this transect (Figure 1d) in general reflects that of the particulate Fe phase.

The enhanced dFe concentrations in the OMZ have been attributed to the remineralization of organic matter plus additional input of Fe from other particulate sources (e.g., atmospheric deposition) [*Fitzsimmons et al.,* 2013; *Rijkenberg et al.,* 2012; *Ussher et al.,* 2013]. A variable relationship between dFe and apparent oxygen utilization (AOU) was observed for each station with r^2 values ranging from 0.3774 to 0.9963. This suggests that remineralization of Fe-containing biogenic particles, while variable, formed an important source of dFe. Calculation of Fe/C ratios by converting AOU to remineralized organic carbon (applying an AOU/C ratio of 1.6 from *Martin et al.* [1989]) yielded Fe/C ratios in the range 8.1–40.6 µmol mol^{-1}. The lower values (8.1–11 µmol mol^{-1}) were representative of open ocean waters and are typical of Fe/C ratios reported for this region of the North Atlantic [*Fitzsimmons et al.,* 2013; *Rijkenberg et al.,* 2014; *Ussher et al.,* 2013]. These values are several fold higher than data from the low-Fe waters of the Pacific Ocean [*Sunda*, 1997], which has been attributed in part to luxury Fe uptake in North Atlantic waters [*Sunda*, 1997]; however, they are up to fourfold lower than reported Fe/C ratios observed in phytoplankton in this region [*Twining et al.,* 2015] and bulk estimates of plankton Fe/C [*Kuss and Kremling*, 1999]. The discrepancy between our calculated Fe/C ratios (8.1–11 µmol mol^{-1}) and the higher observed values is attributed to scavenging and different rates of nutrient remineralization in the water column [*Hatta et al.,* 2015; *Twining et al.,* 2015]. We did however calculate higher Fe/C ratios for shelf-influenced waters (13.3–40.6 µmol mol^{-1}) which are in a similar range to those reported by *Twining et al.* [2015]. These enhanced shelf-influenced Fe/C values reflect additional dFe inputs, either from the shelf sediments and/or dissolution of pFe, or result from faster rates of pFe remineralization relative to C in the more productive shelf waters.

While remineralization is an important source of dFe in this region, the dFe-AOU regression analyses suggest that up to ~60% of the variance in dFe concentrations can be attributed to other sources or processes. Based on the relationship between L-pFe and dFe observed in our dataset, alongside the 20–30% of pFe which is labile and available for dissolution, we hypothesize that while Fe-binding ligands may control the solubility of dFe in the ocean, it is pFe and more specifically the labile fraction (L-pFe) which "buffers" and ultimately controls dFe concentrations. If we therefore consider the L-pFe observed in the OMZ as part of the "available" Fe pool, then at the outer most stations (7–9 and 18) where the influence of the shelf has diminished, this particulate fraction could increase the total available Fe (dFe + L-pFe) by up to 55%.
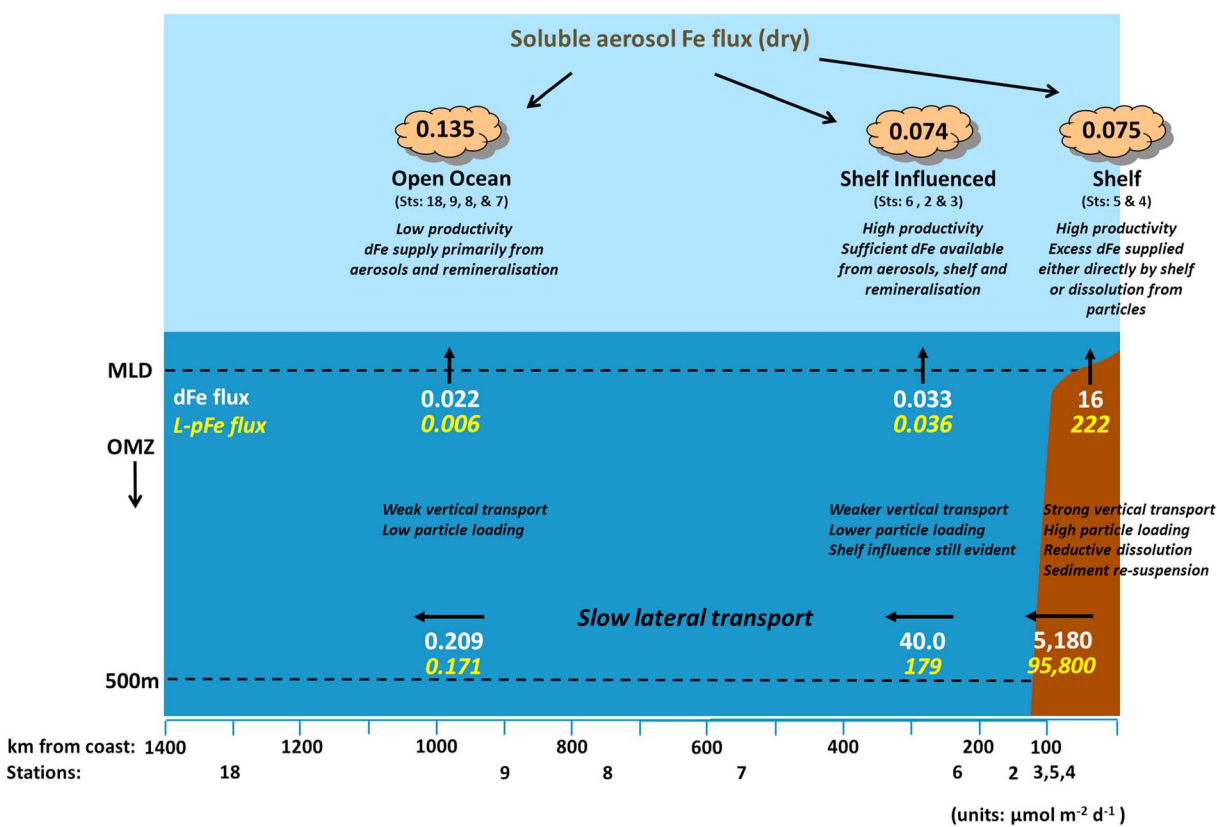
Figure 3. Schematic of Fe fluxes. The nine stations were allocated into a zone (shelf, shelf influenced, and open ocean), and the averaged flux for that zone is shown. Fluxes for dFe are in white and L-pFe in yellow. Values in $\mu mol\,m^{-2}\,d^{-1}$.

3.4. The Significance of Shelf-Derived Fe

The continental shelf in the OMZ of the (sub)-tropical North Atlantic is a distinct source for both particulate and dissolved Fe in this region (Figures 1b and 1d). To further assess the significance of this shelf-derived Fe supply, in comparison with dust deposition in the study area, fluxes for each were determined. Traditionally, only dFe has been accounted for in water column calculations, but as L-pFe can be considered as part of the "available" Fe pool, we have also calculated fluxes for this particulate fraction (see section 2). The differing magnitudes of these fluxes split the transect into three zones: shelf (stations 4 and 5), shelf influenced (stations 3, 2, and 6), and open ocean (stations 7–9 and 18). The dFe and L-pFe fluxes for each of these zones were averaged and are shown along with our average soluble aerosol Fe flux (see section 2), obtained from samples collected during this study from the respective zones (Figure 3). Full details of the estimated dFe and L-pFe fluxes for each station are in the supporting information (Table S2).

The total horizontal flux of Fe was highest in the shelf zone where mean exports of dFe and L-pFe were estimated to be ~5000 and 96,000 $\mu mol\,m^{-2}\,d^{-1}$, respectively. With increasing distance from the coast, the horizontal transport of dFe and L-pFe rapidly decreased, resulting in open ocean zone fluxes of 0.209 and 0.171 $\mu mol\,m^{-2}\,d^{-1}$, respectively. The nearshore lateral transport of dFe is one of the highest reported and is driven by the steep horizontal concentration gradient of dFe observed from the shelf to open ocean waters. Overall, our range of horizontal dFe fluxes for all stations (0.075–6700 $\mu mol\,m^{-2}\,d^{-1}$) are more variable than the range reported for a transect to the north of our study (33–288 $\mu mol\,m^{-2}\,d^{-1}$ [*Rijkenberg et al.,* 2012]). The higher values were closer in magnitude to those reported by *de Jong et al.* [2012] for a Southern Ocean region close to a continental shelf (~1400 $\mu mol\,m^{-2}\,d^{-1}$). Limited data are available for fluxes of particulate material, but our estimates are in agreement with those of *Ratmeyer et al.* [1999]. These workers reported horizontal advection for lithogenic material of $0.1 \times 10^6\,t\,y^{-1}$ off Cape Verde, adjusting this to

include all particulate material (an increase of between 30% and 60% [*Ohnemus and Lam*, 2015]), and assuming that 25% relates to L-pFe, then the flux estimates for our shelf stations were of a similar magnitude. While the horizontal transport of Fe decreased away from the shelf, when combined as one "available" Fe fraction, the flux of dFe and L-pFe (0.380 μmol m^{-2} d^{-1}) in the open ocean zone is greater than our soluble aerosol Fe deposition (0.135 ± 0.085 μmol m^{-2} d^{-1}, $n = 8$). While these fluxes exert influence on different parts of the water column, this comparison reinforces the view that horizontal transport is important in this region and reiterates the emerging view that continental margins are an important supplier of nutrients and trace elements to ocean interiors [*Charette et al.*, 2016; *Lam et al.*, 2006].

For the horizontal Fe flux to impact ocean productivity and/or diazotrophy, vertical transfer into the surface mixed layer must occur. The calculated average vertical supply of dFe was greatest in the shelf zone at 16 μmol m^{-2} d^{-1} and decreased to 0.022 μmol m^{-2} d^{-1} for the open ocean zone. Similarly, the calculated vertical flux of L-pFe decreased over the transect but was more dramatic, decreasing from 222 to 0.006 μmol m^{-2} d^{-1} from shelf to the open ocean zones, respectively. The high vertical mixing in the shelf regions occurred where Fe concentration gradients were steepest, a result of dissolution, turbulence, and sediment remobilization processes enriching overlying bottom waters in both Fe phases (e.g., ~6 nM of dFe and ~31 nM L-pFe). In general the overall concentrations of Fe in the water column were highest in this region, thus providing an enhanced Fe pool for transfer to surface waters. The calculated vertical supply of Fe into the surface mixed layer diminished over the transect, and in the open ocean zone, the dominant supply of Fe to surface waters, with an estimated soluble flux of 0.135 μmol m^{-2} d^{-1} (Figure 3), was aerosol deposition and agrees with the findings of recent studies [*Dammshauser et al.*, 2013; *Ohnemus and Lam*, 2015]. In general, our atmospheric flux estimates are very similar to the 10 year average flux of soluble Fe (0.117 μmol m^{-2} d^{-1}), calculated for our study region during the same sampling period, December to February [*Powell et al.*, 2015]. This seasonal average includes a substantial portion from wet deposition, a component which was not encountered during our own east-west transect but is known to be an important constituent of atmospheric deposition in the (sub)tropical North Atlantic [*Baker et al.*, 2007; *Buck et al.*, 2010; *Schlosser et al.*, 2014]. All atmospheric deposition is known to be highly transient and variable in intensity, and our own dry deposition data show this, where in the 2 week period of sampling between occupation of stations 9 and 18, soluble Fe deposition decreased from 0.145 to 0.011 μmol m^{-2} d^{-1}, respectively. Compiling data from three previous studies that have reported soluble Fe from North African aerosols, and applying the same minimum and maximum deposition velocity used in our own flux calculations, results in an aerosol Fe flux estimate ranging from 0.001 μmol m^{-2} d^{-1} to 4.11 μmol m^{-2} d^{-1} [*Baker et al.*, 2013; *Buck et al.*, 2010; *Trapp et al.*, 2010]. As with any calculations, all of these flux estimates have uncertainties associated with them, and for atmospheric fluxes, dry deposition velocity is a major uncertainty. Uncertainties aside, the lower of these estimates would certainly increase the importance of any additional Fe source to this region. Additionally, the bioavailable Fe fraction from dust is quickly utilized, and its impact on productivity may be short lived (lasting ~2 weeks in studies from the subarctic Pacific [*Bishop et al.*, 2002]). Furthermore, recent studies relating to cellular quotas suggest that Fe availability from dust may be limited and/or have a short residence time [*Ohnemus and Lam*, 2015; *Twining et al.*, 2015], in surface waters of the North Atlantic. During periods of low dust loadings, such as those experienced outside of the winter months [*Powell et al.*, 2015], the potential supply of dFe and L-pFe from below could therefore constitute an additional important source of Fe.

4. Conclusions

Our results show that L-pFe can contribute a significant increase (up to 55%) to the overall "available" Fe pool. The strong relationship between L-pFe and dFe indicates an equilibrium between the two phases, through dissolution and readsorption, whereby L-pFe buffers and maintains the high dFe concentrations observed in the open ocean waters of the OMZ. Lateral flux estimates for L-pFe are of a similar magnitude to dFe and aerosol sources, reinforcing the importance of particle measurements. Particles, and most importantly the labile fraction, are integral to cycling and maintaining Fe bioavailability in the oceans and therefore warrant inclusion in both Fe budgets and biogeochemical models. Given the key role of Fe in controlling oceanic productivity, accurate representations of Fe sources are crucial to predict ocean sensitivity to perturbations in the Fe cycle.

References

Baker, A. R., K. Weston, S. D. Kelly, M. Voss, P. Streu, and J. N. Cape (2007), Dry and wet deposition of nutrients from the tropical Atlantic atmosphere: Links to primary productivity and nitrogen fixation, *Deep Sea Res., Part I*, *54*(10), 1704–1720, doi:10.1016/j.dsr.2007.07.001.

Baker, A. R., C. Adams, T. G. Bell, T. D. Jickells, and L. Ganzeveld (2013), Estimation of atmospheric nutrient inputs to the Atlantic Ocean from 50 degrees N to 50 degrees S based on large-scale field sampling: Iron and other dust-associated elements, *Global Biogeochem. Cycles*, *27*, 755–767, doi:10.1002/gbc.20062.

Berger, C. J. M., S. M. Lippiatt, M. G. Lawrence, and K. W. Bruland (2008), Application of a chemical leach technique for estimating labile particulate aluminum, iron, and manganese in the Columbia River plume and coastal waters off Oregon and Washington, *J. Geophys. Res.*, *113*, C00B01, doi:10.1029/2007JC004703.

Bergquist, B. A., J. Wu, and E. A. Boyle (2007), Variability in oceanic dissolved iron is dominated by the colloidal fraction, *Geochim. Cosmochim. Acta*, *71*(12), 2960–2974, doi:10.1016/j.gca.2007.03.013.

Bishop, J. K. B., R. E. Davis, and J. T. Sherman (2002), Robotic observations of dust storm enhancement of carbon biomass in the North Pacific, *Science*, *298*(5594), 817–821, doi:10.1126/science.1074961.

Boyd, P. W., and M. J. Ellwood (2010), The biogeochemical cycle of iron in the ocean, *Nat. Geosci.*, *3*(10), 675–682, doi:10.1038/ngeo964.

Boyd, P. W., et al. (2012), Microbial control of diatom bloom dynamics in the open ocean, *Geophys. Res. Lett.*, *39*, L18601, doi:10.1029/2012GL053448.

Brand, L. E. (1991), Minimum iron requirements of marine-phytoplankton and the implications for the biogeochemical control of new production, *Limnol. Oceanogr.*, *36*(8), 1756–1771.

Bruland, K. W., K. J. Orians, and J. P. Cowen (1994), Reactive trace metals in the stratified central North Pacific, *Geochim. Cosmochim. Acta*, *58*(15), 3171–3182.

Buck, C. S., W. M. Landing, J. A. Resing, and C. I. Measures (2010), The solubility and deposition of aerosol Fe and other trace elements in the North Atlantic Ocean: Observations from the A16N CLIVAR/CO_2 repeat hydrography section, *Mar. Chem.*, *120*(1-4), 57–70, doi:10.1016/j.marchem.2008.08.003.

Charette, M. A., et al. (2016), Coastal ocean and shelf-sea biogeochemical cycling of trace elements and isotopes: Lessons learned from GEOTRACES, *Philos. Trans. R. Soc. A*, *374*(2081), doi:10.1098/rsta.2016.0076.

Conway, T. M., and S. G. John (2014), Quantification of dissolved iron sources to the North Atlantic Ocean, *Nature*, *511*(7508), 212–215, doi:10.1038/nature13482.

Dammshauser, A., T. Wagener, D. Garbe-Schonberg, and P. Croot (2013), Particulate and dissolved aluminum and titanium in the upper water column of the Atlantic Ocean, *Deep Sea Res., Part I*, *73*, 127–139, doi:10.1016/j.dsr.2012.12.002.

de Jong, J. T. M., V. Schoemann, D. Lannuzel, P. Croot, H. de Baar, and J. L. Tison (2012), Natural iron fertilization of the Atlantic sector of the Southern Ocean by continental shelf sources of the Antarctic Peninsula, *J. Geophys. Res.*, *117*, G01029, doi:10.1029/2011JG001679.

Duce, R. A., R. Arimoto, and B. J. Ray (1986), Atmospheric distribution and sources of trace-metals over the Pacific Ocean, *Atmos. Environ.*, *20*(10), 2073–2074, doi:10.1016/0004-6981(86)90368-9.

Duce, R. A., et al. (1991), The atmospheric input of trace species to the world ocean, *Global Biogeochem. Cycles*, *5*, 193–260, doi:10.1029/91GB01778.

Elrod, V. A., W. M. Berelson, K. H. Coale, and K. S. Johnson (2004), The flux of iron from continental shelf sediments: A missing source for global budgets, *Geophys. Res. Lett.*, *31*, L12307, doi:10.1029/2004GL020216.

Fitzsimmons, J. N., R. F. Zhang, and E. A. Boyle (2013), Dissolved iron in the tropical North Atlantic Ocean, *Mar. Chem.*, *154*, 87–99, doi:10.1016/j.marchem.2013.05.009.

Formenti, P., W. Elbert, W. Maenhaut, J. Haywood, and M. O. Andreae (2003), Chemical composition of mineral dust aerosol during the Saharan Dust Experiment (SHADE) airborne campaign in the Cape Verde region, September 2000, *J. Geophys. Res.*, *108*(D18), 8576, doi:10.1029/2002JD002648.

Ganzeveld, L., J. Lelieveld, and G. J. Roelofs (1998), A dry deposition parameterization for sulfur oxides in a chemistry and general circulation model, *J. Geophys. Res.*, *103*, 5679–5694, doi:10.1029/97JD03077.

Gledhill, M., and C. M. G. van den Berg (1994), Determination of complexation of iron(III) with natural organic complexing ligands in seawater using cathodic stripping voltammetry, *Mar. Chem.*, *47*(1), 41–54.

Glover, D. M., W. J. Jenkins, and S. C. Doney (2011), *Modeling Methods for Marine Science*, Cambridge Univ. Press, Cambridge, U. K., doi:10.1017/CBO9780511975721.

Hatta, M., C. I. Measures, J. Wu, S. Roshan, J. N. Fitzsimmons, P. Sedwick, and P. Morton (2015), An overview of dissolved Fe and Mn distributions during the 2010–2011 U.S. GEOTRACES North Atlantic cruises: GEOTRACES GA03, *Deep Sea Res., Part II*, *116*, 117–129, doi:10.1016/j.dsr2.2014.07.005.

Homoky, W. B., S. Severmann, J. McManus, W. M. Berelson, T. E. Riedel, P. J. Statham, and R. A. Mills (2012), Dissolved oxygen and suspended particles regulate the benthic flux of iron from continental margins, *Mar. Chem.*, *134*, 59–70, doi:10.1016/j.marchem.2012.03.003.

Hong, H. S., and D. R. Kester (1986), Redox state of iron in the offshore waters of Peru, *Limnol. Oceanogr.*, *31*(3), 512–524.

Hurst, M. P., A. M. Aguilar-Islas, and K. W. Bruland (2010), Iron in the southeastern Bering Sea: Elevated leachable particulate Fe in shelf bottom waters as an important source for surface waters, *Cont. Shelf Res.*, *30*(5), 467–480, doi:10.1016/j.csr.2010.01.001.

Jickells, T. D. (1999), The inputs of dust derived elements to the Sargasso Sea; a synthesis, *Mar. Chem.*, *68*(1–2), 5–14.

Jickells, T. D., et al. (2005), Global iron connections between desert dust, ocean biogeochemistry, and climate, *Science*, *308*(5718), 67–71.

John, S. G., and J. Adkins (2012), The vertical distribution of iron stable isotopes in the North Atlantic near Bermuda, *Global Biogeochem. Cycles*, *26*, GB2034, doi:10.1029/2011GB004043.

Klunder, M. B., P. Laan, R. Middag, H. J. W. De Baar, and J. C. van Ooijen (2011), Dissolved iron in the Southern Ocean (Atlantic sector), *Deep Sea Res., Part II*, *58*(25-26), 2678–2694, doi:10.1016/j.dsr2.2010.10.042.

Kuss, J., and K. Kremling (1999), Spatial variability of particle associated trace elements in near-surface waters of the North Atlantic (30 degrees N/60 degrees W to 60 degrees N/2 degrees W), derived by large-volume sampling, *Mar. Chem.*, *68*(1–2), 71–86, doi:10.1016/s0304-4203(99)00066-3.

Lam, P. J., and J. K. B. Bishop (2008), The continental margin is a key source of iron to the HNLC North Pacific Ocean, *Geophys. Res. Lett.*, *35*, L07608, doi:10.1029/2008GL033294.

Lam, P. J., J. K. B. Bishop, C. C. Henning, M. A. Marcus, G. A. Waychunas, and I. Y. Fung (2006), Wintertime phytoplankton bloom in the subarctic Pacific supported by continental margin iron, *Global Biogeochem. Cycles*, *20*, GB1006, doi:10.1029/2005GB002557.

Lam, P. J., D. C. Ohnemus, and M. E. Auro (2015), Size-fractionated major particle composition and concentrations from the US GEOTRACES north Atlantic zonal transect, *Deep Sea Res., Part II*, *116*, 303–320, doi:10.1016/j.dsr2.2014.11.020.

Lippiatt, S. M., M. T. Brown, M. C. Lohan, C. J. M. Berger, and K. W. Bruland (2010), Leachable particulate iron in the Columbia River, estuary, and near-field plume, *Estuarine Coastal Shelf Sci.*, *87*(1), 33–42, doi:10.1016/j.ecss.2009.12.009.

Lippiatt, S. M., M. T. Brown, M. C. Lohan, and K. W. Bruland (2011), Reactive iron delivery to the Gulf of Alaska via a Kenai eddy, *Deep Sea Res., Part I*, *58*(11), 1091–1102, doi:10.1016/j.dsr.2011.08.005.

Maldonado, M. T., and N. M. Price (1996), Influence of N substrate on Fe requirements of marine centric diatoms, *Mar. Ecol. Prog. Ser.*, *141*(1–3), 161–172.

Marchetti, A., M. T. Maldonado, E. S. Lane, and P. J. Harrison (2006), Iron requirements of the pennate diatom *Pseudo-nitzschia*: Comparison of oceanic (high-nitrate, low-chlorophyll waters) and coastal species, *Limnol. Oceanogr.*, *51*(5), 2092–2101.

Martin, J. H., R. M. Gordon, S. Fitzwater, and W. W. Broenkow (1989), Vertex: Phytoplankton/iron studies in the Gulf of Alaska, *Deep Sea Res., Part I*, *36*(5), 649–680.

McLennan, S. M. (2001), Relationships between the trace element composition of sedimentary rocks and upper continental crust, *Geochem. Geophys. Geosyst.*, *2*, 1021, doi:10.1029/2000GC000109.

Morel, F. M. M., A. J. Milligan, and M. A. Saito (2003), 6.05 - Marine bioinorganic chemistry: The role of trace metals in the oceanic cycles of major nutrients, in *Treatise on Geochemistry*, edited by H. D. Holland and K. K. Turekian, pp. 113–143, Pergamon, Oxford, U. K.

Neuer, S., V. Ratmeyer, R. Davenport, G. Fischer, and G. Wefer (1997), Deep water particle flux in the Canary Island region: Seasonal trends in relation to long-term satellite derived pigment data and lateral sources, *Deep Sea Res., Part I*, *44*(8), 1451–1466, doi:10.1016/s0967-0637(97)00034-4.

Obata, H., H. Karatani, and E. Nakayama (1993), Automated determination of iron in seawater by chelating resin concentration and chemi-luminescence detection, *Anal. Chem.*, *65*(11), 1524–1528.

Ohnemus, D. C., and P. J. Lam (2015), Cycling of lithogenic marine particles in the US GEOTRACES North Atlantic transect, *Deep Sea Res., Part II*, *116*, 283–302, doi:10.1016/j.dsr2.2014.11.019.

Ohnemus, D. C., M. E. Auro, R. M. Sherrell, M. Lagerstrom, P. L. Morton, B. S. Twining, S. Rauschenberg, and P. J. Lam (2014), Laboratory intercomparison of marine particulate digestions including Piranha: A novel chemical method for dissolution of polyethersulfone filters, *Limnol. Oceanogr. Methods*, *12*, 530–547, doi:10.4319/lom.2014.12.530.

Okubo, A. (1971), Oceanic diffusion diagrams, *Deep Sea Res.*, *18*(8), 789–802, doi:10.1016/0011-7471(71)90046-5.

Powell, C. F., A. R. Baker, T. D. Jickells, H. W. Bange, R. J. Chance, and C. Yodle (2015), Estimation of the atmospheric flux of nutrients and trace metals to the eastern tropical North Atlantic Ocean, *J. Atmos. Sci.*, *72*(10), 4029–4045, doi:10.1175/jas-d-15-0011.1.

Ratmeyer, V., G. Fischer, and G. Wefer (1999), Lithogenic particle fluxes and grain size distributions in the deep ocean off northwest Africa: Implications for seasonal changes of aeolian dust input and downward transport, *Deep Sea Res., Part I*, *46*(8), 1289–1337, doi:10.1016/s0967-0637(99)00008-4.

Revels, B. N., D. C. Ohnemus, P. J. Lam, T. M. Conway, and S. G. John (2015), The isotope signature and distribution of particulate iron in the North Atlantic Ocean, *Deep Sea Res., Part II*, *116*, 321–331, doi:10.1016/j.dsr2.2014.12.004.

Rhein, M., M. Dengler, J. Sueltenfuss, R. Hummels, S. Huettl-Kabus, and B. Bourles (2010), Upwelling and associated heat flux in the equatorial Atlantic inferred from helium isotope disequilibrium, *J. Geophys. Res.*, *115*, C08021, doi:10.1029/2009JC005772.

Rijkenberg, M. J. A., S. Steigenberger, C. F. Powell, H. van Haren, M. D. Patey, A. R. Baker, and E. P. Achterberg (2012), Fluxes and distribution of dissolved iron in the eastern (sub-) tropical North Atlantic Ocean, *Global Biogeochem. Cycles*, *26*, 15, doi:10.1029/2011GB004264.

Rijkenberg, M. J. A., R. Middag, P. Laan, L. J. A. Gerringa, H. M. van Aken, V. Schoemann, J. T. M. de Jong, and H. J. W. de Baar (2014), The distribution of dissolved iron in the West Atlantic Ocean, *PLoS One*, *9*(6), 14, doi:10.1371/journal.pone.0101323.

Rudnick, R. L., and S. Gao (2003), 3.01 - The composition of the continental crust, in *Treatise on Geochemistry*, edited by H. D. Holland, and K. K. Turekian, pp. 1–64, Pergamon, Oxford, U. K., doi:10.1016/B0-08-043751-6/03016-4.

Rue, E. L., and K. W. Bruland (1995), Complexation of iron(III) by natural organic-ligands in the central North Pacific as determined by a new competitive ligand equilibration adsorptive cathodic stripping voltammetric method, *Mar. Chem.*, *50*(1–4), 117–138.

Schlosser, C., J. K. Klar, B. D. Wake, J. T. Snow, D. J. Honey, E. M. S. Woodward, M. C. Lohan, E. P. Achterberg, and C. M. Moore (2014), Seasonal ITCZ migration dynamically controls the location of the (sub)tropical Atlantic biogeochemical divide, *Proc. Natl. Acad. Sci. U.S.A.*, *111*(4), 1438–1442, doi:10.1073/pnas.1318670111.

Shelley, R. U., P. L. Morton, and W. M. Landing (2015), Elemental ratios and enrichment factors in aerosols from the US-GEOTRACES North Atlantic transects, *Deep Sea Res., Part II*, *116*, 262–272, doi:10.1016/j.dsr2.2014.12.005.

Stramma, L., and F. Schott (1999), The mean flow field of the tropical Atlantic Ocean, *Deep Sea Res., Part II*, *46*(1-2), 279–303, doi:10.1016/s0967-0645(98)00109-x.

Stramma, L., S. Huttl, and J. Schafstall (2005), Water masses and currents in the upper tropical northeast Atlantic off northwest Africa, *J. Geophys. Res.*, *110*, C12006, doi:10.1029/2005JC002939.

Stramma, L., P. Brandt, J. Schafstall, F. Schott, J. Fischer, and A. Kortzinger (2008), Oxygen minimum zone in the North Atlantic south and east of the Cape Verde Islands, *J. Geophys. Res.*, *113*, C04014, doi:10.1029/2007JC004369.

Sunda, W. G. (1997), Control of dissolved iron concentrations in the world ocean: A comment, *Mar. Chem.*, *57*(3-4), 169–172.

Sunda, W. G. (2001), Bioavailability and bioaccumulation of iron in the sea, in *The Biogeochemistry of Iron in Seawater*, edited by D. R. Turner and K. A. Hunter, pp. 41–84, John Wiley, Chichester, England.

Sunda, W. G., D. G. Swift, and S. A. Huntsman (1991), Low iron requirement for growth in oceanic phytoplankton, *Nature*, *351*(6321), 55–57, doi:10.1038/351055a0.

Tagliabue, A., J. B. Sallee, A. R. Bowie, M. Levy, S. Swart, and P. W. Boyd (2014), Surface-water iron supplies in the Southern Ocean sustained by deep winter mixing, *Nat. Geosci.*, *7*(4), 314–320, doi:10.1038/ngeo2101.

Trapp, J. M., F. J. Millero, and J. M. Prospero (2010), Trends in the solubility of iron in dust-dominated aerosols in the equatorial Atlantic trade winds: Importance of iron speciation and sources, *Geochem. Geophys. Geosyst.*, *11*, Q03014, doi:10.1029/2009GC002651.

Twining, B. S., S. Rauschenberg, P. L. Morton, and S. Vogt (2015), Metal contents of phytoplankton and labile particulate material in the North Atlantic Ocean, *Prog. Oceanogr.*, *137*, 261–283, doi:10.1016/j.pocean.2015.07.001.

Ussher, S. J., E. P. Achterberg, C. Powell, A. R. Baker, T. D. Jickells, R. Torres, and P. J. Worsfold (2013), Impact of atmospheric deposition on the contrasting iron biogeochemistry of the North and South Atlantic Ocean, *Global Biogeochem. Cycles*, *27*, 1096–1107, doi:10.1002/gbc.20056.

Wedepohl, K. H. (1995), The composition of the continental crust, *Geochim. Cosmochim. Acta*, *59*(7), 1217–1232, doi:10.1016/0016-7037(95)00038-2.

Wells, M. L., N. M. Price, and K. W. Bruland (1995), Iron chemistry in seawater and its relationship to phytoplankton - A workshop report, *Mar. Chem.*, *48*(2), 157–182.

Whitfield, M. (2001), Interactions between phytoplankton and trace metals in the ocean, in *Advances in Marine Biology*, vol 41, edited by A. J. Southward, et al., pp. 1–128, Academic Press, New York, doi:10.1016/s0065-2881(01)41002-9.

Wu, J. F., and G. W. Luther (1994), Size-fractionated iron concentrations in the water column of the western North-Atlantic Ocean, *Limnol. Oceanogr.*, *39*(5), 1119–1129.